The σ-phase superconductors $Nb_{20.4}Rh_{5.7}Ge_{3.9}$ and $Nb_{20.4}Rh_{5.7}Si_{3.9}$

Elizabeth M. Carnicom[a], Tai Kong[a], Tomasz Klimczuk[b], R.J. Cava[a],

[a]*Department of Chemistry, Princeton University, Princeton, New Jersey 08544*

[b] *Department of Physics, Gdansk University of Technology, Gdansk 80-233, Poland*

Abstract

We show that the previously unreported ternary σ phases $Nb_{20.4}Rh_{5.7}Ge_{3.9}$ and $Nb_{20.4}Rh_{5.7}Si_{3.9}$ are both superconductors with Tc values of approximately 1.9 K. The superconducting transitions were characterized through temperature-dependent magnetic susceptibility, electrical resistance, and specific heat measurements. The Sommerfeld constants, γ, for $Nb_{20.4}Rh_{5.7}Ge_{3.9}$ and $Nb_{20.4}Rh_{5.7}Si_{3.9}$ are 89(1) mJ mol-f.u.$^{-1}$ K^{-2} and 86(1) mJ mol-f.u.$^{-1}$ K^{-2} (about 3.0 and 2.9 mJ mol-atom^{-1} K^{-2}), respectively. The normalized specific heat jumps at T_c, $\Delta C/\gamma T_c$, are approximately 1.39 for $Nb_{20.4}Rh_{5.7}Ge_{3.9}$ and 1.30 for $Nb_{20.4}Rh_{5.7}Si_{3.9}$, consistent with both materials being weakly coupled BCS type superconductors.

1. Introduction

Intermetallic sigma (σ) phases crystallize in the tetragonal space group $P4_2/mnm$ (No. 136) with the CrFe-structure-type. With 30 atoms per unit cell and five inequivalent crystallographic sites: 2a, 4f, $8i_1$, $8i_2$, and 8j [1–6], σ phases are relatively complex, with topologically closest packed structures belonging to the Frank-Kasper [7–11] family of phases. The atoms in σ phases are coordinated by three of the four possible Frank-Kasper polyhedra with coordination numbers of 15 (4f), 14, ($8i_1$ and 8j), and 12 (2a and $8i_2$). Other important characteristics of σ phases are their non-stoichiometric atom ratios and also their tolerance for a wide range of compositions. The result is that the crystal structures can have high degrees of substitutions on the different

crystallographic sites – binary and ternary sigma phases are known [1,2,6,12–19]. These hard, brittle transition metal alloys have been studied in particular because the precipitation of σ phases can result in deleterious effects on the mechanical properties of steel such as embrittlement or the loss of resistance to corrosion [20–23].

Many binary σ phases have been reported to display superconductivity. For example, $Mo_{0.63}Ru_{0.37}$ is a superconductor with a Tc of ~7K [24,25] and the critical temperature of $Nb_{0.62}Pt_{0.38}$ is 2.1 K [26]. The wide composition ranges that are characteristic of σ phases often result in equally wide ranges in Tc. For example, in the Nb-Ir binary system, the T_c of the σ phases can range from 2 to 9 K based on the material's composition [24,27–30]. In general, previous work has shown that as the composition is varied, Tc increases with decreasing unit cell volume and increasing valence electron count per atom [24,31]. Due to the large number of reported σ phase superconductors, this structure-type, in spite of its complexity, can be considered a promising host for superconductivity.

Here we report the two ternary σ phase superconductors $Nb_{20.4}Rh_{5.7}Ge_{3.9}$ and $Nb_{20.4}Rh_{5.7}Si_{3.9}$. To the best of our knowledge, $Nb_{20.4}Rh_{5.7}Ge_{3.9}$ [32] is the only other known ternary σ phase superconductor. In addition, the phases NbRhGe and NbRhSi seem to be the only other phases to exist in the Nb-Rh-Ge and Nb-Rh-Si systems [33,34]. (Deviations from the complex atomic ratios of 20.4:5.7:3.9 results in the presence of secondary phases in all three cases.) A Rietveld refinement with occupancies fixed to those previously reported for the Nb-Ru-Ge σ phase (but with Rh in place of the Ru) resulted in a structural model that is in good agreement with the observed diffraction data for $Nb_{20.4}Rh_{5.7}Ge_{3.9}$. $Nb_{20.4}Rh_{5.7}Si_{3.9}$ had broader diffraction peaks, suggesting the presence of smaller grain size or some composition variation in this material compared to $Nb_{20.4}Rh_{5.7}Ge_{3.9}$. The superconducting transitions of $Nb_{20.4}Rh_{5.7}Ge_{3.9}$ and

$Nb_{20.4}Rh_{5.7}Si_{3.9}$ are sharp and reproducible across multiple experiments. Temperature-dependent magnetic susceptibility, electrical resistance, and specific heat measurements were used to characterize the superconducting critical temperature for each superconducting σ phase to be about 1.9 K. Specific heat measurements confirmed that both materials are bulk superconductors.

2. Experimental

The starting materials for synthesis of the polycrystalline samples of the $Nb_{20.4}Rh_{5.7}Si_{3.9}$ and $Nb_{20.4}Rh_{5.7}Ge_{3.9}$ superconductors were elemental niobium (> 99.9%, 325 mesh, Aldrich), rhodium (99.9%, bullion, Baird & Co. Bullion Merchants), germanium (> 99.9%, 3.2 mm, Alfa Aesar), and silicon (> 99.9%, lump, 15 cm, Alfa Aesar). Both materials were prepared in a similar way to $Nb_{20.4}Rh_{5.7}Ge_{3.9}$ [32]. Niobium powder was pressed into a pellet using a hydraulic press and then arc-melted to create a single niobium metal piece for subsequent melting with germanium (or silicon) and rhodium. The niobium, rhodium and germanium (or silicon) pieces were then placed in an arcmelter under 600 mbar of a Zr-gettered Ar atmosphere and were melted together three times in a 20.4:5.7:3.9 ratio and flipped over in between each melting to ensure homogeneity. Small amounts of impurity phases were present when the loading composition deviated by 0.3 from the molar ratio 20.4:5.7:3.9 and significant impurities resulted for deviations above 0.3. The resulting arc-melted buttons had<1% mass loss and the samples are stable in air. The Ge-variant was wrapped in Ta foil, sealed in an evacuated silica tube, and annealed at 1100 °C for 24 h to obtain the purest phase with the sharpest diffraction peaks; the quality of the Si-variant did not increase upon annealing. The purity of each sample was checked using a room temperature powder X-ray Bruker D8 Advance Eco Cu Kα radiation (λ=1.5406 Å) diffractometer using a LynxEye-XE detector. A Rietveld refinement for $Nb_{20.4}Rh_{5.7}Ge_{3.9}$ was performed using the FullProf Suite with Thompson-Cox-Hastings pseudo-Voigt peak shapes. Lattice parameters from the single

crystal refinement of isostructural $Nb_{20.4}Rh_{5.7}Ge_{3.9}$ [32] were used as a starting point. The chemical formulas were constrained to $Nb_{20.4}Rh_{5.7}Ge_{3.9}$ and $Nb_{20.4}Rh_{5.7}Si_{3.9}$ since the diffraction patterns were single phase and there was<1% mass loss after arc-melting the samples. VESTA [35] was used to create the crystal structure image.

A Quantum Design Physical Property Measurement System (PPMS) Dynacool with a vibrating sample magnetometer (VSM) option was used to measure the zero-field cooled (ZFC) and field-cooled (FC) temperature-dependent magnetic susceptibility from 1.68 K–2.3 K for $Nb_{20.4}Rh_{5.7}Ge_{3.9}$ and $Nb_{20.4}Rh_{5.7}Si_{3.9}$ with a H=10 Oe applied magnetic field. The field-dependent magnetization was measured at 1.68 K from 0 to 150 Oe. The PPMS equipped with a resistivity option was used to measure the temperature-dependent electrical resistance using a standard four-probe method from 300 K to 1.7 K with a 1 mA applied current. The specific heat was measured on small samples (~10 mg) of $Nb_{20.4}Rh_{5.7}Ge_{3.9}$ and $Nb_{20.4}Rh_{5.7}Si_{3.9}$ from 6 K to 1.8 K under zero applied magnetic field using Apiezon N grease.

3. Results and discussion

There are no previously reported σ phases in the Nb-Ge, Nb-Si, Rh-Ge, or Rh-Si binary systems, but a binary σ phase superconductor $Nb_{0.65}Rh_{0.35}$ is known [36]. Room temperature powder X-ray diffraction data (pXRD) showed that both our previously unreported ternary materials, superconducting $Nb_{20.4}Rh_{5.7}Ge_{3.9}$ and $Nb_{20.4}Rh_{5.7}Si_{3.9}$, crystallize in the tetragonal space group P42/*mnm* (No. 136) with the CrFe structure type typical of σ phases. We saw no evidence for a solid solution between these materials and the binary Nb-Rh σ phase; precise ternary compositions are needed to synthesize single phase materials. The lattice parameters are a=9.8484(1) Å and c=5.1300(1) Å for $Nb_{20.4}Rh_{5.7}Ge_{3.9}$ and a=9.8107(2) Å and c=5.1238(1) Å for

$Nb_{20.4}Rh_{5.7}Si_{3.9}$, respectively. Table 1 shows the results of the Rietveld refinement for $Nb_{20.4}Rh_{5.7}Ge_{3.9}$, where the site occupancies were fixed to the values determined previously [32] for the isostructural superconductor $Nb_{20.4}Rh_{5.7}Ge_{3.9}$ (though with Rh in place of the Ru). This model gave an exceptional fit to the data, as seen in Fig. 1a. A LeBail fit was used for $Nb_{20.4}Rh_{5.7}Si_{3.9}$ (Fig. 1b) because the cluster of high intensity peaks near 40° 2θ had wider peaks than those seen for the Ge variant: the diffraction peaks for this material suggest that it may have either a smaller grain size or some composition variation when compared to the Ge variant. To most quantitatively determine the site occupancies of both $Nb_{20.4}Rh_{5.7}Ge_{3.9}$ and $Nb_{20.4}Rh_{5.7}Si_{3.9}$, diffraction at multiple wavelengths of radiation (with different atomic scattering factors) would be required, which is beyond the scope of the present study. For the current purposes, it is sufficient to confirm that our materials are single phase, and that their diffraction patterns index to the space group P42/*mnm* (No. 136) and display peak intensities to indicate that they are isostructural with other previously reported σ phases. Fig. 1c shows the crystal structure of $Nb_{20.4}Rh_{5.7}Ge_{3.9}$ viewed along the c-direction, emphasizing its topologically closest packed structure.

To characterize the superconducting T_c, the field-dependent volume magnetization (MV) and temperature-dependent volume magnetic susceptibility (χ_V) were measured for both $Nb_{20.4}Rh_{5.7}Ge_{3.9}$ (Fig. 2a) and for $Nb_{20.4}Rh_{5.7}Si_{3.9}$ (Fig. 2b). The MV was measured from 0 to 150 Oe for both $Nb_{20.4}Rh_{5.7}Ge_{3.9}$ (Fig. 2a, inset) and $Nb_{20.4}Rh_{5.7}Si_{3.9}$ (Fig. 2b, inset) at 1.68 K and fitted with the equation $M_{fit} = bH + a$, where b is the slope of the fitted line. The equation, $-b = \frac{1}{4\pi(1-N)}$ was then used to determine the demagnetization factor, N, for each sample, which is based on the sample shape and how the sample is oriented with respect to the applied magnetic field. The N values obtained (N=0.348 and 0.359, for the Ge and Si variants, respectively) were used to correct the magnetic susceptibility data in the main panels of Fig. 2a–b. Both zerofield cooled (ZFC) and

field cooled (FC) $\chi_V(T)$ were measured from 1.68 K–2.3 K with H=10 Oe as the applied magnetic field for both $Nb_{20.4}Rh_{5.7}Ge_{3.9}$ and $Nb_{20.4}Rh_{5.7}Si_{3.9}$. The resulting diamagnetic signal at 1.68 K is very close to the ideal value of $4\pi\chi_V(1\text{-}N)=-1$ for both superconductors. The intersection of the extrapolated normal state susceptibility with the steepest slope of the diamagnetic superconducting signal (black solid lines) was used to determine the T_c values [37] for the new superconductors to be 1.95 K and 1.91 K for $Nb_{20.4}Rh_{5.7}Ge_{3.9}$ and $Nb_{20.4}Rh_{5.7}Si_{3.9}$, respectively. Polycrystalline samples typically have weak signals in FC measurements, as is seen in our materials.

Table 1. Atomic coordinates of $Nb_{20.4}Rh_{5.7}Ge_{3.9}$ from the Rietveld refinement of room temperature powder X-ray diffraction data[a] in space group $P4_2/mnm$, with a = 9.8484(1) Å and c = 5.1300(1) Å.

Atom	Wyckoff Position	Occupancy[b]	*x*	*y*	*z*	B_{iso}
Rh/Ge1/Nb4	2*a*	0.67/0.23/0.1	0	0	0	3.3(1)
Rh/Ge2/Nb5	8*j*	0.54/0.43/0.025	0.1816(1)	0.1816(1)	0.2522(5)	2.46(3)
Nb1	4*f*	1	0.3962(2)	0.3962(2)	0	3.10(7)
Nb2	$8i_2$[c]	1	0.7405(3)	0.0674(3)	0	3.42(4)
Nb3	$8i_1$[c]	1	0.4637(2)	0.1278(2)	0	3.23(5)

[a] Rietveld agreement factors: $\chi^2 = 2.67$; $wR_p = 15.3\%$; $R_p = 15.5\%$; $R(F^2) = 9.38\%$.
[b] The occupancies were fixed to values observed previously from a single crystal refinement of $Nb_{20.4}Ru_{5.7}Ge_{3.9}$ [32].
[c] Describing the 8*i* sites as $8i_1$ and $8i_2$ is convention for σ phases. See Ref. [2].

The temperature-dependent normalized resistance R/R_{300K} is shown in Fig. 3a for $Nb_{20.4}Rh_{5.7}Ge_{3.9}$ and Fig. 3b for $Nb_{20.4}Rh_{5.7}Si_{3.9}$. The resistance remains relatively flat throughout the entire temperature range above T_c for both materials -they are "poor metals" presumably due to the substitutional disorder present. These data are consistent with what is observed for the other ternary σ phase superconductor $Nb_{20.4}Rh_{5.7}Ge_{3.9}$ [32]. The insets of Fig. 3a–b show the resistance dropping to zero at ~1.9 K for both materials, consistent with the observed T_c values obtained from the temperature-dependent magnetic susceptibility measurements.

The temperature-dependent specific heat was measured under zero applied magnetic field in the vicinity of the superconducting transitions or $Nb_{20.4}Rh_{5.7}Ge_{3.9}$ (Fig. 4a) and $Nb_{20.4}Rh_{5.7}Si_{3.9}$ (Fig. 4b) and plotted as Cp/T vs T. Equal-entropy constructions (yellow shading) of the idealized specific heat jump (solid black lines) were used to determine the T_c to be 1.95 K for the Ge variant and 1.91 K for the Si variant. The large jumps in specific heat are sharp and consistent with bulk superconductivity in both $Nb_{20.4}Rh_{5.7}Ge_{3.9}$ and $Nb_{20.4}Rh_{5.7}Si_{3.9}$.

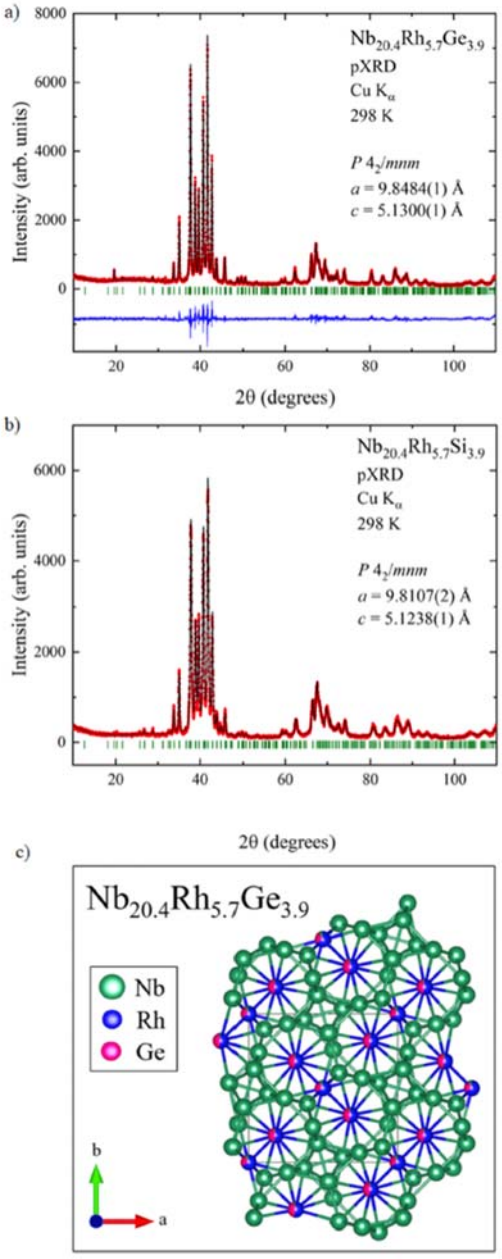

Fig. 1. a) Rietveld structure refinement of the σ-phase $Nb_{20.4}Rh_{5.7}Ge_{3.9}$ from room temperature pXRD data. Red circles - experimentally obtained data, black line - calculated pattern, green vertical bars - expected Bragg reflections, blue line - difference between the observed and calculated data. b) Room temperature pXRD data showing a LeBail fit of the isostructural σ phase $Nb_{20.4}Rh_{5.7}Si_{3.9}$. The group of high intensity peaks near $2\theta = 40°$ is a common feature of σ phases. c) Crystal structure of the topologically closest packed σ phase $Nb_{20.4}Rh_{5.7}Ge_{3.9}$ when viewed along the c-direction, generated from the cif file from the Rietveld refinement of $Nb_{20.4}Rh_{5.7}Ge_{3.9}$. Niobium atoms - green, rhodium atoms - blue, germanium atoms - pink.

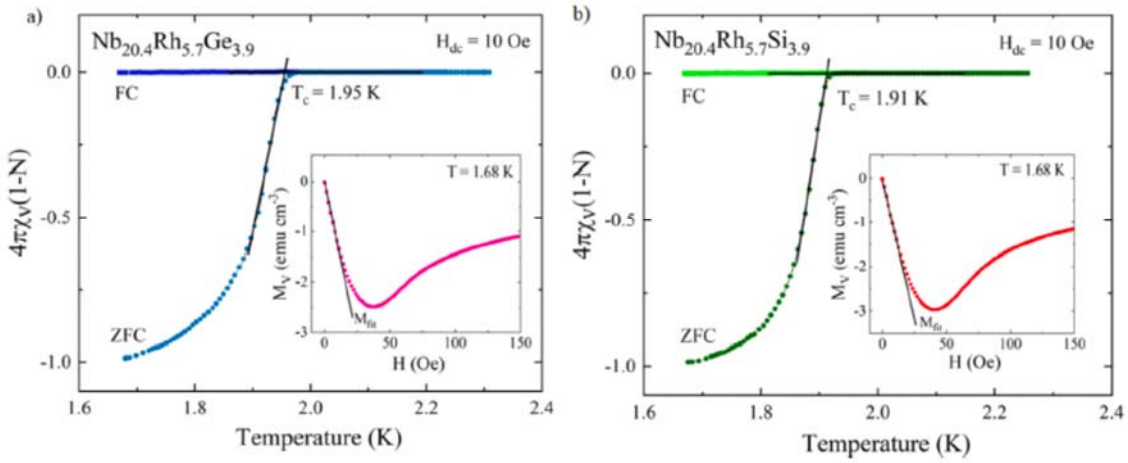

Fig. 2. ZFC and FC temperature dependent magnetic susceptibility $\chi_V(T)$ for a) $Nb_{20.4}Rh_{5.7}Ge_{3.9}$ and b) $Nb_{20.4}Rh_{5.7}Si_{3.9}$ measured in a H = 10 Oe applied magnetic field from 1.68 K–2.3 K and corrected for the demagnetization factor, N. The ZFC measurements show a superconducting critical temperature of a) 1.95 K and b) 1.91 K. Inset: Field-dependent magnetization data measured at 1.68 K for a) $Nb_{20.4}Rh_{5.7}Ge_{3.9}$ and b) $Nb_{20.4}Rh_{5.7}Si_{3.9}$ to estimate the value of the demagnetization factor, N, for each sample based on the fit line, M_{fit}.

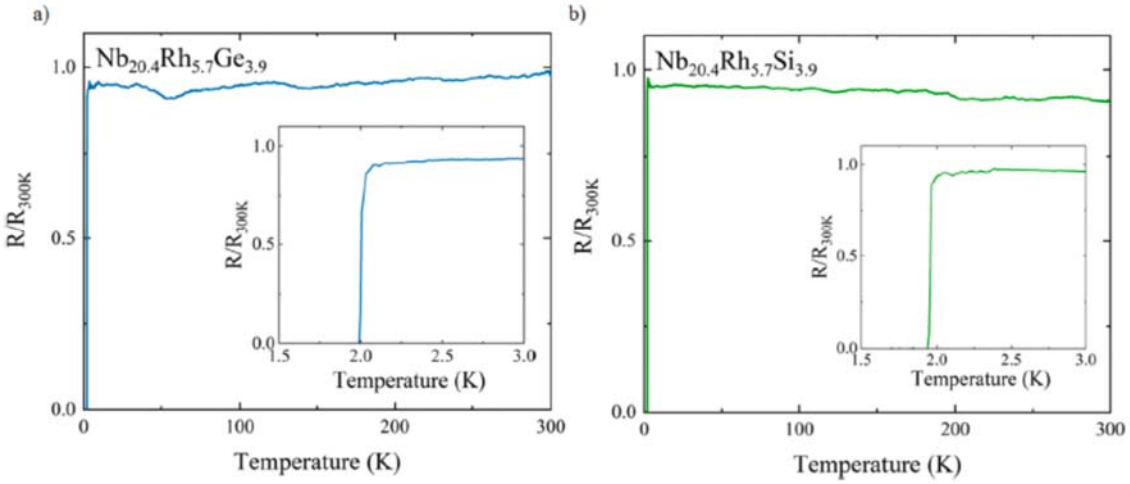

Fig. 3. Temperature-dependent normalized electrical resistance, R/R_{300K} for a) $Nb_{20.4}Rh_{5.7}Ge_{3.9}$ and b) $Nb_{20.4}Rh_{5.7}Si_{3.9}$ between 300 K–1.7 K under zero applied magnetic field. Inset: R/R_{300K} for a) $Nb_{20.4}Rh_{5.7}Ge_{3.9}$ and b) $Nb_{20.4}Rh_{5.7}Si_{3.9}$ from 1.5 K–3.0 K showing the superconducting transition at ~1.9 K for each material.

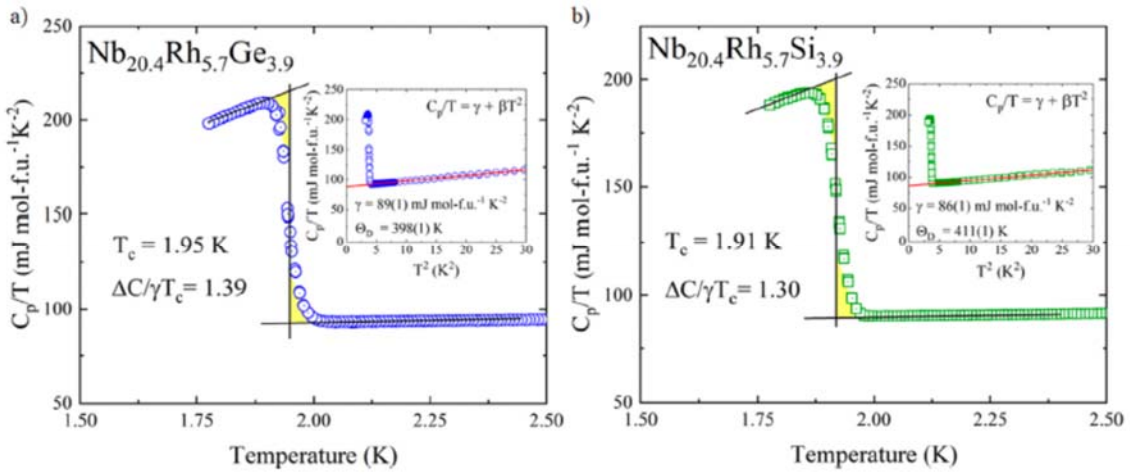

We note that the loss of a significant amount of entropy at a superconducting transition is an unambiguous signature of bulk superconductivity. Our specific heat data, along with the T_c's and

the single phase nature of the materials therefore clearly distinguish our ternary phases from the superconducting Nb-Rh binary phase, whose T_c is 2.9 K [36].

The T_c determined for each superconductor is consistent across the three measurements: magnetic susceptibility, electrical resistance, and specific heat. The insets of Fig. 4a–b shows a plot of C_p/T vs T^2. The data were fitted in the normal state (above T_c) to the equation

$$\frac{C_p}{T} = \gamma + \beta T^2$$

where γT is the electronic contribution and βT 3 the phonon contribution to the specific heat. The slopes of the fitted line, β, were calculated to be 0.921(3) mJ mol-f.u.$^{-1}$K^{-4} and 0.837(3) mJ mol-f.u.$^{-1}$K^{-4} (f.u.=formula unit) for the Ge and Si variant, respectively. The Sommerfeld parameter γ was then calculated to be 89(1) mJ mol-f.u.$^{-1}$K^{-4} and 86(1) mJ mol-f.u.$^{-1}$K^{-4} for $Nb_{20.4}Rh_{5.7}Ge_{3.9}$ and $Nb_{20.4}Rh_{5.7}Si_{3.9}$. The Sommerfeld parameter of the previously reported superconductor $Nb_{20.4}Rh_{5.7}Ge_{3.9}$ was 91(1) mJ mol-f.u.$^{-1}$K^{-2} [32], which is only slightly higher than the values reported here for $Nb_{20.4}Rh_{5.7}Ge_{3.9}$ and $Nb_{20.4}Rh_{5.7}Si_{3.9}$. The Debye temperature (ΘD) for each superconductor was then calculated to be 398(1) K and 411(1) K for $Nb_{20.4}Rh_{5.7}Ge_{3.9}$ and $Nb_{20.4}Rh_{5.7}Si_{3.9}$ using the equation

$$\Theta_D = \left(\frac{12\pi^4}{5\beta} nR\right)^{\frac{1}{3}}$$

where n=30 ($Nb_{20.4}Rh_{5.7}Ge_{3.9}$ or $Nb_{20.4}Rh_{5.7}Si_{3.9}$) and R is the ideal gas constant (R=8.314 J mol^{-1} K^{-1}). The electron-phonon coupling constant λ_{ep} was then calculated to be 0.480 for the Ge variant and 0.475 for the Si variant by using the inverted McMillan formula [38].

$$\lambda_{ep} = \frac{1.04 + \mu * \ln\left(\frac{\Theta_D}{1.45T_c}\right)}{(1 - 0.62\mu *)\ln\left(\frac{\Theta_D}{1.45T_c}\right) - 1.04}$$

together with the values of ΘD, T_c, and assuming that $\mu^* = 0.13$. Based on the λ_{ep} values, both $Nb_{20.4}Rh_{5.7}Ge_{3.9}$ and $Nb_{20.4}Rh_{5.7}Si_{3.9}$ are weak coupling superconductors. The Fermi energy N(EF) was then calculated to be 26 states eV−1 per formula unit of $Nb_{20.4}Rh_{5.7}Ge_{3.9}$ and 25 states eV^{-1} per formula unit of $Nb_{20.4}Rh_{5.7}Si_{3.9}$using the above equation where γ=89(1) mJ mol-f.u.$^{-1}K^{-2}$ for the Ge variant and γ=86(1) mJ mol-f.u.$^{-1}K^{-2}$ for the Si variant. The normalized specific heat jump value, $\Delta C/\gamma T_c$, for $Nb_{20.4}Rh_{5.7}Ge_{3.9}$ is 1.39, which is close to the weak coupling limit based on BCS theory ($\Delta C/\gamma T_c$=1.43) [39]. The $\Delta C/\gamma T_c$ value of $Nb_{20.4}Rh_{5.7}Si_{3.9}$is 1.30, which is slightly less than that observed for the Ge variant. However, the value for each specific heat jump confirms bulk superconductivity in the σ phases $Nb_{20.4}Rh_{5.7}Ge_{3.9}$ and $Nb_{20.4}Rh_{5.7}Si_{3.9}$.

4. Conclusions

We report two new ternary σ phase superconductors $Nb_{20.4}Rh_{5.7}Ge_{3.9}$ and $Nb_{20.4}Rh_{5.7}Si_{3.9}$, which are shown to crystallize in the CrFe structure-type using room-temperature powder X-ray diffraction data; the Si variant appears to be the first Si-containing σ phase superconductor. Each superconductor shows a transition to the superconducting state at ∼1.9 K in its magnetic susceptibility, electrical resistance, and specific heat data. Calculated superconducting parameters confirm that both $Nb_{20.4}Rh_{5.7}Ge_{3.9}$ and $Nb_{20.4}Rh_{5.7}Si_{3.9}$ are weak coupling BCS type superconductors. These materials add to the only other previously reported ternary σ phase superconductor, $Nb_{20.4}Rh_{5.7}Ge_{3.9}$ [32]. The lower Tc for $Nb_{20.4}Rh_{5.7}Ge_{3.9}$ (1.9 K) with its higher electron count per atom than $Nb_{20.4}Rh_{5.7}Ge_{3.9}$ (T_c=2.9 K) is contrary to the general trend seen in superconducting binary σ phases, where increased electron counts lead to higher T_c's, and the essentially equal T_c's for the Si and Ge variants reported here reflect a relative insensitivity of the superconductivity to the identity of the metalloid atoms. Our results show that σ phases continue to be a promising family of materials for hosting superconductivity.

Acknowledgments

The materials synthesis was supported by the Department of Energy, Division of Basic Energy Sciences, Grant DE-FG02-98ER45706, and the property characterization was supported by the Gordon and Betty Moore Foundation EPiQS initiative, Grant GBMF-4412. The research in Poland was supported by the National Science Centre, Grant UMO-2016/22/M/ST5/00435.

References

[1] E.O. Hall, S.H. Algie, The sigma phase, Metall. Rev. 11 (1966) 61–88, https://doi.org/10.1179/mtlr.1966.11.1.61.

[2] J.M. Joubert, Crystal chemistry and Calphad modeling of the σ phase, Prog. Mater. Sci. 53 (2008) 528–583, https://doi.org/10.1016/j.pmatsci.2007.04.001.

[3] D.P. Shoemaker, B.G. Bergman, The crystal structure of a sigma phase, FeCr1, J. Am. Chem. Soc. 72 (1950), https://doi.org/10.1021/ja01168a550 5793–5793.

[4] J.S. Kasper, B.F. Decker, J.R. Belanger, The crystal structure of the sigma-phase in the Co-Cr system, J. Appl. Phys. 22 (1951) 361–362, https://doi.org/10.1063/1.1699960.

[5] G. Bergman, D.P. Shoemaker, The determination of the crystal structure of the σ phase in the iron-chromium and iron-molybdenum systems, Acta Crystallogr. 7 (1954) 857–865, https://doi.org/10.1107/S0365110X54002605.

[6] K. Yaqoob, J.C. Crivello, J.M. Joubert, Comparison of the site occupancies determined by combined Rietveld refinement and density functional theory calculations: example of the ternary Mo-Ni-Re σ-phase, Inorg. Chem. 51 (2012) 3071–3078, https://doi.org/10.1021/ic202479y.

[7] S. Andersson, Structures related to the β- tungsten or Cr3Si structure type, J. Solid State Chem. 23 (1978) 191–204, https://doi.org/10.1016/0022-4596(78)90065-8.

[8] E.I. Gladyshevskii, O. Bodak, Topologically close-packed structures, in: J.H. Westbrook, R.L. Fleischer (Eds.), Intermet. Compd. Princ. Pract, J. Wiley & Sons, Chichester, 1995, pp. 403–418.

[9] J.S. Kasper, R.M. Waterstrat, Ordering of atoms in the σ phase, Acta Crystallogr. 9 (1956) 289–295, https://doi.org/10.1107/S0365110X56000802.

[10] F.C. Frank, J.S. Kasper, Complex alloy structures regarded as sphere packings. II. Analysis and classification of representative structures, Acta Crystallogr. 12 (1959) 483–499, https://doi.org/10.1107/S0365110X59001499.

[11] F.C. Frank, J.S. Kasper, Complex alloy structures regarded as sphere packings. I. Definitions and basic principles, Acta Crystallogr. 11 (1958) 184–190, https://doi.org/10.1107/S0365110X58000487.

[12] I.M. Subbotin, M.V. Raevskaya, T.P. Loboda, E.M. Sokolovskaya, The reaction of molybdenum and ruthenium with transition metals of period VI, Moscow, Univ. Chem. Bull. 36 (1981) 51–54.

[13] Y.I. Gladyshevskiy, L.K. Borusevich, The ternary Cr-Fe-Si system, Russ. Metall. (1966) 87–90 1966.

[14] K.P. Gupta, N.S. Rajan, P.A. Beck, Effect of Si and Al on the stability of certain sigma phases, Trans. Metall. Soc. AIME 218 (1960) 617–624.

[15] J. Tobola, M. Francois, E. Elkaim, J.M. Joubert, M. Vilasi, Resonant X-ray diffraction study and electronic structure calculations of three Mo-Ru-Si ternary phases, Intermetallics 18 (2010) 781–790, https://doi.org/10.1016/j.intermet.2009.12.009.

[16] M.T. Orillion, A. Raman, Alloy chemistry of σ (β-U)- related phases IV. A15, σ', and χ' phases in ternary alloys of refractory metals with gallium, Z. Met. 65 (1974) 709–713.

[17] H. Martens, P. Duwez, Phase relationships in the iron-chromium-vanadium system, Trans. Am. Soc. Met. 44 (1952) 484–493.

[18] A. Bezinge, K. Yvon, J. Müller, Study of A15 and sigma phase alloys in the Nb-V-Ga system, J. Less-Common Met. 98 (1984) L9–L12, https://doi.org/10.1016/0022-5088(84)90290-X.

[19] C.R.J. Hunt, A. Raman, Alloy Chemistry of σ(β-U)-related phases. I. Extension of μ- and occurrence of μ''-phases in the ternary systems Nb (Ta) –X–Al (X = Fe, Co, Ni, Cu, Cr, Mo), Zeitschrift Für Met. 59 (1968) 701–707.

[20] C.-C. Hsieh, W. Wu, Overview of intermetallic sigma (σ) phase precipitation in stainless steels, ISRN Metall. 2012 (2012) 1–16, https://doi.org/10.5402/2012/732471.

[21] L.K. Singhal, J.W. Martin, The formation of ferrite and sigma-phase in some austenitic stainless steels, Acta Metall. 16 (1968) 1441–1451, https://doi.org/10. 1016/0001-6160(68)90039-4.

[22] J. Hau, A. Seijas, Sigma phase embrittlement of stainless steel in FCC service, Corros. Nacexpo 61st Annu. Conf. Expo, 2006, pp. 1–22.

[23] A.D. Warren, R.L. Harniman, Z. Guo, C.M. Younes, P.E.J. Flewitt, T.B. Scott, Quantification of sigma-phase evolution in thermally aged 2205 duplex stainless steel, J. Mater. Sci. 51 (2016) 694–707, https://doi.org/10.1007/s10853-015-9131-9.

[24] R.D. Blaugher, J.K. Hulm, Superconductivity in the σ- and α- Mn structures, J. Chem. Solids 19 (1961) 134–138, https://doi.org/10.1016/0022-3697(61)90067-1.

[25] S.E. Rasmussen, B. Lundtoft, New crystal data for Mo.63Ru.37 (Mo5Ru3) a superconducting sigma phase, Powder Diffr. 2 (1987) 29–30, https://doi.org/10.1017/S0885715600012197.

[26] H.R. Khan, C.J. Raub, K. Lüders, Z. Szücs, Comparison of superconducting Parameters of A 15- and σ-phases of Nb-Pt, Appl. Phys. 15 (1978) 307–313, https://doi.org/10.1007/BF00896113.

[27] V.B. Compton, E. Corenzqit, J.P. Maita, B.T. Matthias, F.J. Morin, Superconductivity of technetium alloys and compounds, Phys. Rev. 123 (1961) 1567–1568, https://doi.org/10.1103/PhysRev.123.1567.

[28] E. Bucher, F. Heininger, J. Müller, Proceedings of the eighth international conference on low temperature physics, Proc. Eighth Int. Conf. Low Temp. Phys, Butterworths, Washington, DC, 1962, p. 153.

[29] H.R. Khan, C.J. Raub, K. Lüders, Z. Szücs, Comparison of superconducting and electronic properties of σ-and A-15 phase Nb-Al, Appl. Phys. 13 (1977) 123–129, https://doi.org/10.1007/BF00882469.

[30] H.R. Khan, C.J. Raub, K. Lüders, Z. Szücs, Superconductivity of A15- and σ-phase of Nb-Ir, Appl. Phys. 19 (1979) 231–235, https://doi.org/10.1007/BF00932403.

[31] R.D. Blaugher, A. Taylor, J.K. Hulm, The superconductivity of some intermetallic compounds, IBM J. Res. Dev. 6 (1962) 116–118, https://doi.org/10.1147/rd.61.0116.

[32] E.M. Carnicom, W.W. Xie, Z. Sobczak, T. Kong, T. Klimczuk, R.J. Cava, Superconductivity in the Nb-Ru-Ge σ-phase, Phys. Rev. Mater. 1 (2017) 074802, https://doi.org/10.1103/PhysRevMaterials.1.074802.

[33] S. Yashiro, A. Kasahi, R. Kasai, H. Samata, Y. Nagata, New equiatomic silicides of MM'Si (M=Nb, Ta; M' = Pt, Rh) and superconductivity of Ta1-xNbxPtSi, J. Alloy. Compd. 309 (2000) 51–56.

[34] V. Johnson, W. Jeitschko, Ternary equiatomic transition metal silicides and germanides, J. Solid State Chem. 4 (1972) 123–130, https://doi.org/10.1016/0022-4596(72)90140-5.

[35] K. Momma, F. Izumi, VESTA 3 for three-dimensional visualization of crystal, volumetric and morphology data, J. Appl. Crystallogr. 44 (2011) 1272–1276, https://doi.org/10.1107/S0021889811038970.

[36] H.R. Khan, K. Lüders, C.J. Raub, G. Roth, Superconductivity and resistance behavior of σ -phase alloys: Nb-Rh and Ta-Rh, Z. Phys. B Condens. Matter 38 (1980) 27–33, https://doi.org/10.1007/BF01321199.

[37] T. Klimczuk, R.J. Cava, Carbon isotope effect in superconducting MgCNi3, Phys. Rev. B 70 (2004) 212514, https://doi.org/10.1103/PhysRevB.70.212514.

[38] W.L. McMillan, Transition temperature of strong-coupled superconductors, Phys. Rev. 167 (1968) 331–344, https://doi.org/10.1103/PhysRev.167.331.

[39] M. Tinkham, Introduction to Superconductivity, second ed., Dover Publications, Inc, Mineola, 1996.